Noncovalent Synthesis of Melamine−Cyanuric/Barbituric Acid Derived Nanostructures: Regio- and Stereoselection

Peter Timmerman,*[a] Leonard J. Prins[a]

Keywords: Chirality / Noncovalent interactions / Self-assembly / Supramolecular chemistry / Stereoselection

The hydrogen bond directed self-assembly of calix[4]arene dimelamines and barbituric or cyanuric acid derivatives gives ready access to organic nanostructures of nanometer dimensions. The synthesis, characterization, and supramolecular chirality of these noncovalent assemblies are discussed in detail, together with means of achieving regio-, diastereo-, and enantioselection. Self-organizing behaviour into higher order aggregates on solid surfaces is also described.

1. Introduction and Stimulus

Organic chemists have been studying the making and breaking of covalent bonds as a way to synthesize new molecules for more than a century. The approach has proved to be extremely fruitful for the synthesis of molecules with molecular weights in the range of 100−3000 Da; some examples that spring to mind are the total syntheses of impressive chemical structures such as palytoxin,[1] taxol,[2] or norbrevetoxin.[3,4] However, it may now be that *covalent synthesis* has reached the limits of what is synthetically feasible in terms of time requirements and yields,[5] and it follows that the investment of time and effort necessary to construct monodisperse functional nanoscale structures of 10−100 kDa MW using this approach has to be viewed as prohibitive.

Nowadays, *noncovalent synthesis* is increasingly being considered as a potential alternative for the construction of chemical nanostructures incorporating a high degree of complexity.[6,7] One major advantage over covalent synthesis is that noncovalent assembly formation is often reversible, meaning that the assembled structures are "proofread" and, where necessary, corrected for unstable "errors". Obviously, noncovalent assemblies are much less robust than covalent structures, which means that their isolation and manipulation deserves special attention. As always, inspiration comes from biological systems, in which functioning noncovalent nanoscale structures are constructed and modified with startling efficiency. Illustrative examples include duplex DNA, α-hemoglobin (the oxygen-carrying hemoprotein consists of four identical subunits), and the tobacco mosaic virus (TMV), a right-handed helical filament made up of 2,130 identical subunits.[8] Similarly, it is

[a] Department of Supramolecular Chemistry & Technology, MESA+ Research Institute, University of Twente
P. O. Box 217, 7500 AE Enschede, The Netherlands
E-mail: p.timmermann@ct.utwente.nl

Peter Timmerman (left) was born in Ommen, The Netherlands in 1966. He received his degree in chemistry in 1989 with G. W. Klumpp at the Free University in Amsterdam. In 1994 he obtained his PhD at the University of Twente (UT) with D. N. Reinhoudt (summa cum laude), working on the synthesis of rigid cavities by combination of calix[4]arenes and resorcinarenes, for which he was awarded the Backer Prize. He then moved to a postdoctoral position with F. N. Diederich at the Eidgenössische Technische Hochschule (ETH) in Zürich, Switzerland, working on the chemistry of fullerenes. Since 1995 he has been back at the University of Twente, where he is Universitair Docent in the group of D. N. Reinhoudt. His current research interests centre around the various aspects of self-assembly based on hydrogen bonding and ionic interactions, with a particular focus on noncovalent combinatorial synthesis.

Leonard Prins (right), born in 1974, studied Chemical Technology at the University of Twente, The Netherlands. He obtained his undergraduate degree in 1996 with D. N. Reinhoudt. In 1997, after spending three months in the group of R. Ungaro in Parma, Italy, he rejoined the Reinhoudt group as a graduate student. His research deals with the noncovalent synthesis of chiral hydrogen-bonded assemblies.

MICROREVIEWS: This feature introduces the readers to the authors' research through a concise overview of the selected topic. Reference to important work from others in the field is included.

  1434−193X/01/0917−3191 $ 17.50+.50/0

possible to build synthetic nanostructures by utilizing multiple noncovalent interactions that may act in a cooperative manner. Different types of interactions have been used for this purpose, the major ones being metal coordination,[9,10] hydrogen bonding,[6] and ionic[11] and hydrophobic interactions.[12,13]

2. The Cyanuric Acid·Melamine (CA·M) Motif: Rosettes versus Tapes

2.1. The CA·M Lattice

Part of the research in our group is concerned with the noncovalent synthesis of hydrogen-bonded nanostructures based on interactions between cyanuric acid (CA) and melamine (M). Complementary hydrogen bond formation between cyanuric acid (CA) and melamine (M) in the CA·M lattice[14] is among the best-studied structural motifs for self-assembly of linear and cyclic hydrogen-bonded assemblies.[15–18] The hydrogen bond directed assembly of cyanurate and melamine derivatives can in principle give rise to three different types of aggregates: the (finite) cyclic *rosettes*,[17,18] the (infinite) *linear tapes*,[15,19] and the (infinite) *crinkled tapes* (see Figure 1, a).[20] From Whitesides' seminal work on hydrogen-bonded assemblies, two general concepts for the preferential formation of cyclic rosettes have emerged.[7] The concept of *covalent preorganization* (Figure 1, b) uses a Hub-spacer (C_3 symmetry) to preorganize the individual melamine units in a cyclic fash-

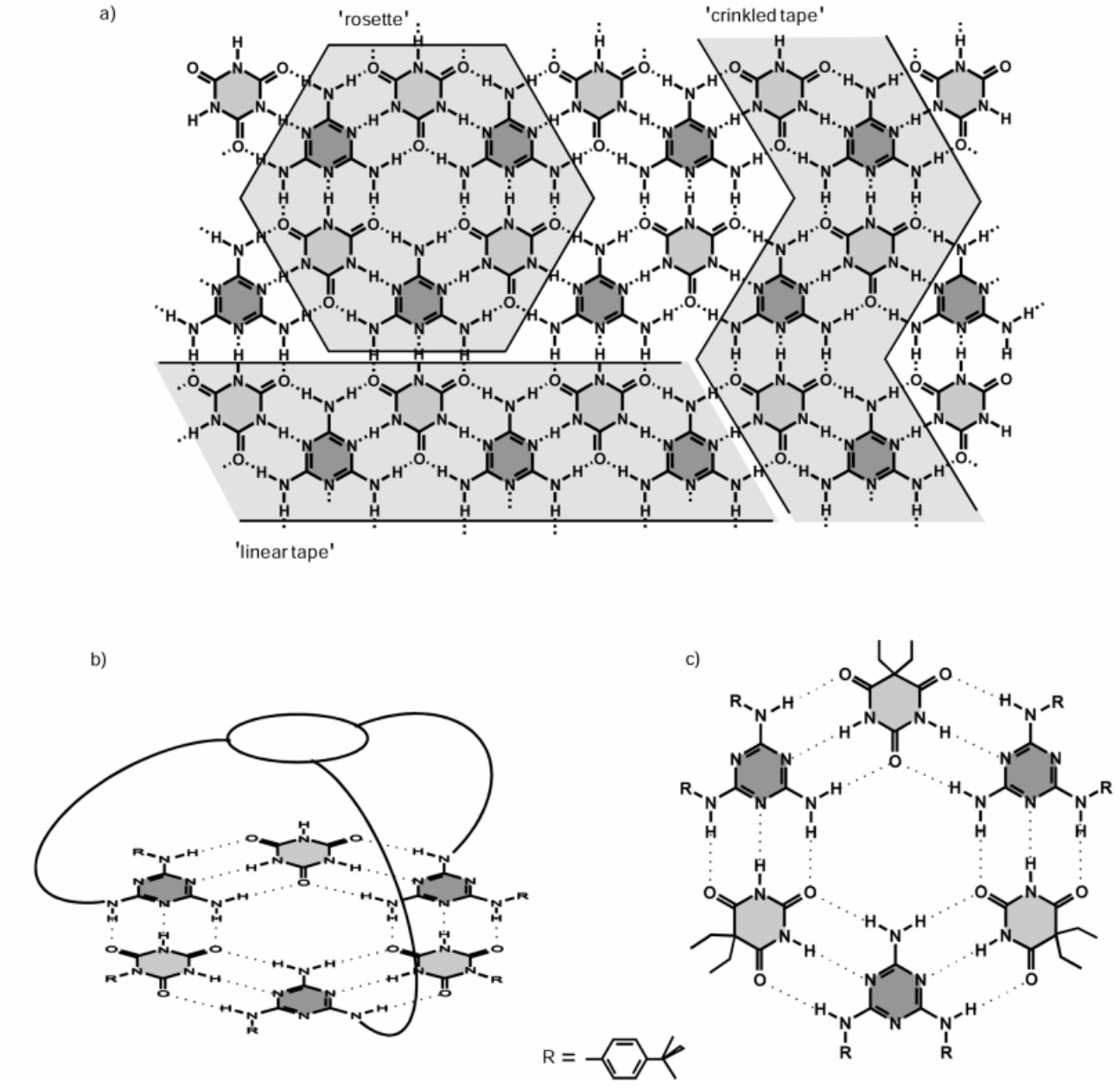

Figure 1. a) Assembly motif: melamine·cyanuric acid (M·CA); selective formation of the cyclic rosette motif using the concepts of b) covalent preorganization or c) peripheral crowding

ion.[16] The concept of *peripheral crowding* (Figure 1, c) is based on the fact that melamines with sterically bulky substituents promote single rosette formation through the introduction of unfavourable steric interactions in the corresponding tape-like structures.[17,21,22]

2.2. Evaluation of the Concept of Peripheral Crowding

We have recently developed a model that describes the self-assembly of melamine and cyanuric acid derivatives into rosettes and tapes.[23] The model considers all possible stereoisomeric tape structures up to eight different components (270 different species) and one cyclic rosette structure. Furthermore, it takes into account all the different types of steric interactions within the assemblies. Calculations using this model have shown that the repulsive steric interactions in linear tapes *hardly affect the composition of the equilibrium mixture*. It was found that the rosette fraction in an equilibrating mixture of *N*,*N*-disubstituted melamines and *N*-substituted cyanuric acid derivatives changes from 25% to only 41% when all possible steric interactions that can occur in the tapes are included ($[CA]_0 = [M]_0 = 10^{-2}$ M). In sharp contrast to this, calculations clearly show that parameters directly affecting the thermodynamic stability of the rosette strongly influence the rosette fraction in the mixture. For example, an increase in K_0 (the basic equilibrium constant for a single CA·M interaction) from 100 to 10 000 M^{-1} causes an increase in the rosette fraction *from* $\leqslant$ *5% to 90%*. Similarly, an increase in K_r, a parameter that characterizes the equilibrium between linear and cyclic hexamer, from 0.001 to 0.1 M also increases the rosette fraction *from ca. 10% to 85%* ($[CA]_0 = [M]_0 = 10^{-2}$ M).[24,25] These results do not support the concept of peripheral crowding as put forward by Whitesides,[17,21,22] but clearly show that steric interactions play only a minor role in the self-assembly process. The observed preference for rosette formation in the solid state in the case of sterically bulky melamines is most probably due to large differences in the solubility of rosette and the tape-like structures, but does not seem to reflect their thermodynamic stability in solution.

3. Self-Assembly of Calix[4]arenes through Multiple Hydrogen Bond Formation

3.1. Calix[4]arene Double Rosettes

Five years ago we started a research program on "the noncovalent synthesis of molecular receptors using hydrogen bonding". As a recognition motif we selected the CA·M moiety, because of its synthetic accessibility and high degree of controllability. We found that calix[4]arenes diametrically substituted with two melamine units at the upper rim form well-defined, box-like assemblies in the presence of 2 equiv. of 5,5-disubstituted barbituric acid (BAR) or *N*-substituted cyanuric acid (CYA) derivatives.[26,27] These assemblies consist of three calix[4]arene dimelamines and six DEB or CYA units, held together by a total of 36 hydrogen bonds (see Scheme 1). The top and bottom of this assembly comprise cyclic hydrogen-bonded platforms, with the calix[4]arene units acting as side walls.

In principle, these assemblies can exist in three isomeric forms: the D_3 isomer (*staggered*), which is chiral (vide infra), the C_{3h} isomer, and the C_s isomer (both *eclipsed*) (Figure 2). In the *staggered* isomer the two melamines of each calix[4]arene unit are in an *antiparallel* orientation with respect to each other, while in the *eclipsed* isomers both melamines are parallel. The C_{3h} isomer and the C_s isomer differ only in the orientation of one single calix[4]arene unit, which is rotated by 180° on going from one isomer to the other. Experimentally, only the D_3 isomer has been observed for $\mathbf{1}_3$·$(DEB)_6$, while all three isomers have been observed for $\mathbf{1}_3$·$(CYA)_6$ assemblies, the relative ratio being strongly dependent on the peripheral substituents of the individual components.[28]

3.2. Characterization of Double Rosette Assemblies

Noncovalent assemblies are generally far less robust than covalent structures. For this reason, their structural characterization is far from straightforward and special techniques to prove their formation are often needed. This section briefly discusses important techniques that have been used in our laboratories for the structural characterization of hydrogen-bonded assemblies, in particular the double rosette assemblies.

^{1}*H NMR Spectroscopy*

Calix[4]arene double rosettes can conveniently be characterized by ^{1}H NMR spectroscopy. Highly diagnostic are the imide NH proton signals, which are usually observed between $\delta = 13$ and 16, a region free of other resonances. The D_3 and the C_{3h} isomers give two signals for the imide NH protons, while for the C_s isomer all the imide NH protons are different, and consequently give six different signals.

The spectrum of assembly $\mathbf{1}_3$·$(DEB)_6$ in $CDCl_3$ clearly shows that the assembly exists exclusively as one single conformational isomer (the D_3 isomer) (Figure 3, a). The hydrogen-bonded NH protons of DEB give rise to two signals, at $\delta = 14.10$ and 13.32. That these proton signals are observed at different chemical shifts is a result of the unsymmetrical substitution of the melamine units, which renders the two protons chemically distinct in the assembly. Two additional signals appear at $\delta = 8.37$ (c) and 7.43 (d), corresponding to the two secondary amine protons of **1**. Two signals are observed for the two NH_2 protons, at $\delta \approx 6.9$ (e) and 6.7 (f). The aromatic protons *ortho* to the melamine substituents of the calix[4]arene **1** resonate at very different frequencies, at $\delta = 7.15$ (g) and 6.03 (h). In free **1**, these protons display broad signals at $\delta = 6.65-6.05$. At a 1:2 ratio of **1**/DEB, the spectrum is sharp and does not display residual signals for **1**. When more than 2 equiv. of DEB are added, a broad signal for the NH protons of free DEB is observed alongside the two signals for hydrogen-bonded DEB.

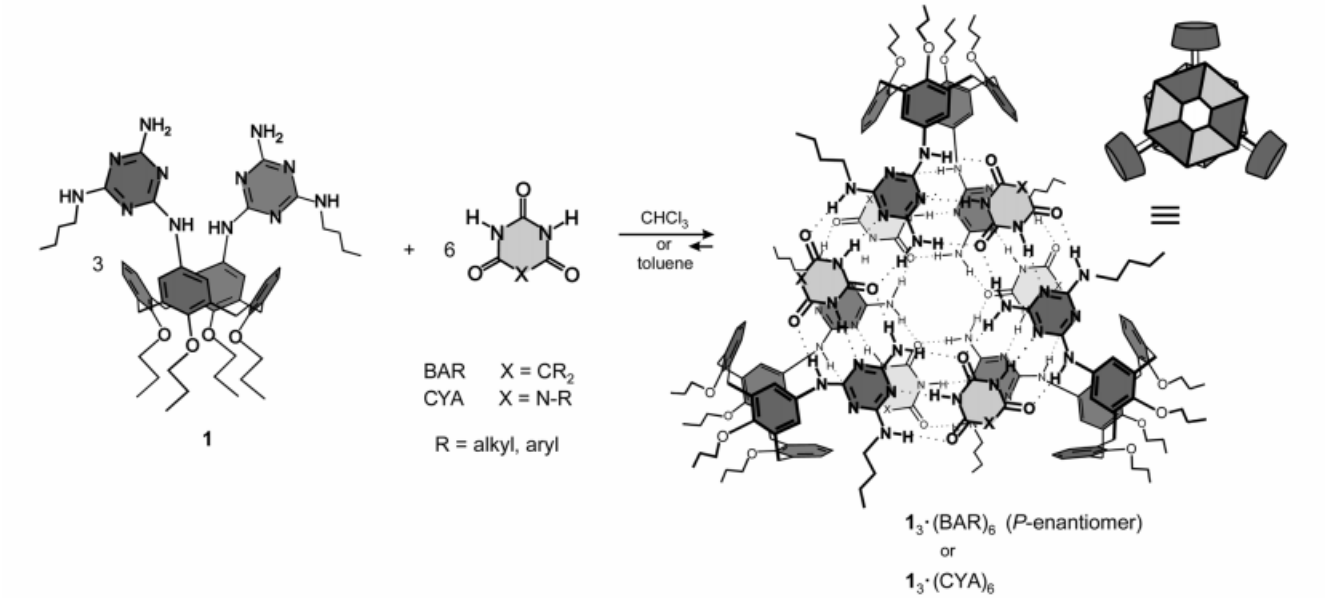

Scheme 1. Noncovalent synthesis of double rosette assemblies $\mathbf{1}_3$·(DEB)$_6$ or $\mathbf{1}_3$·(CYA)$_6$

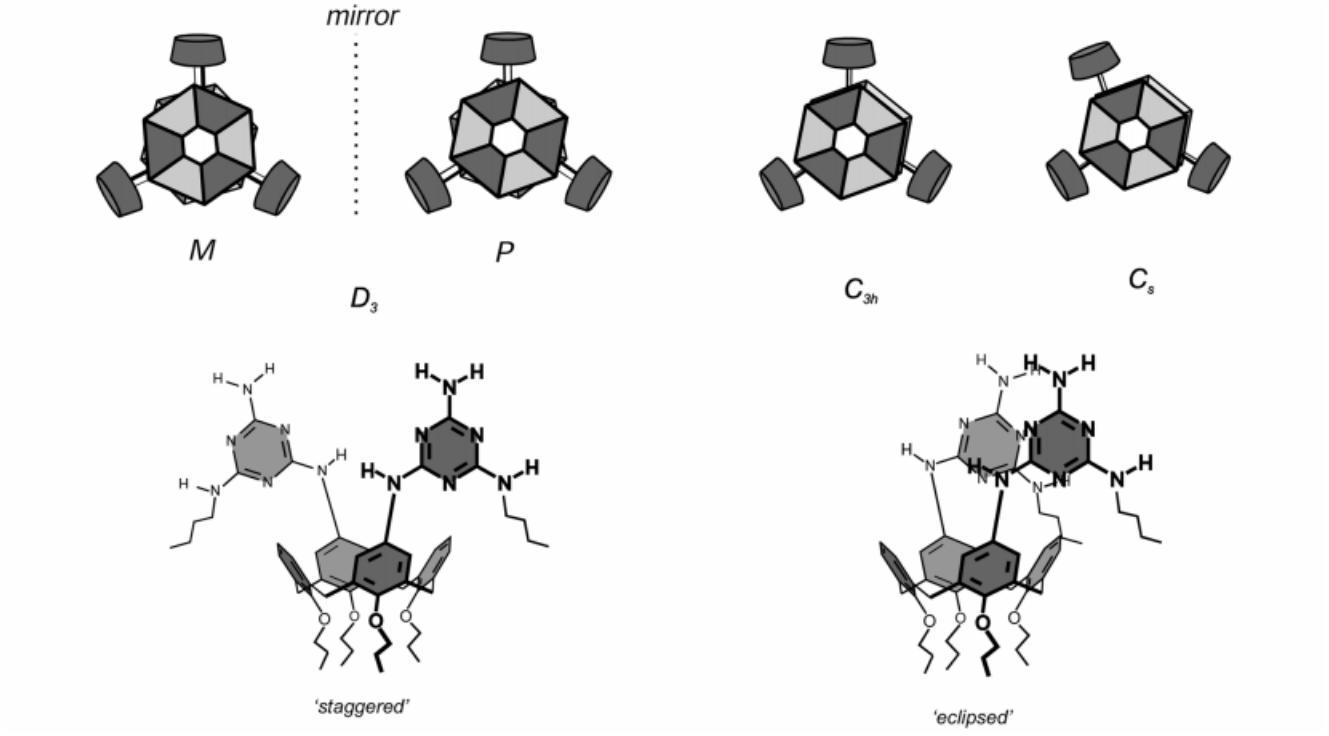

Figure 2. Conformational isomerism in calix[4]arene double rosette assemblies

In collaboration with Cohen's group (Tel Aviv University, Israel), we have recently studied our rosette assemblies using NMR diffusion spectroscopy. The method provides information on the diffusion rates of the assemblies, which relates well to their size and structure. In a number of cases, these measurements gave conclusive evidence about the identity of the assemblies.[29]

UV Spectroscopy

In collaboration with Wurthner's group (University of Ulm, Germany), we have studied double rosette assemblies incorporating the chromogenic barbiturate (DπA)-BAR. Upon formation of the assembly, the barbiturates undergo a small but significant hypsochromic shift (14 nm), which makes it possible to observe both the assembly and the free components separately. This provides a unique opportunity to study the assembly process by UV at μM concentrations (see Section 3.3).[30]

CD Spectroscopy

Thanks to the chiral orientation of the melamine and cyanurate components within the assembly, we have been in-

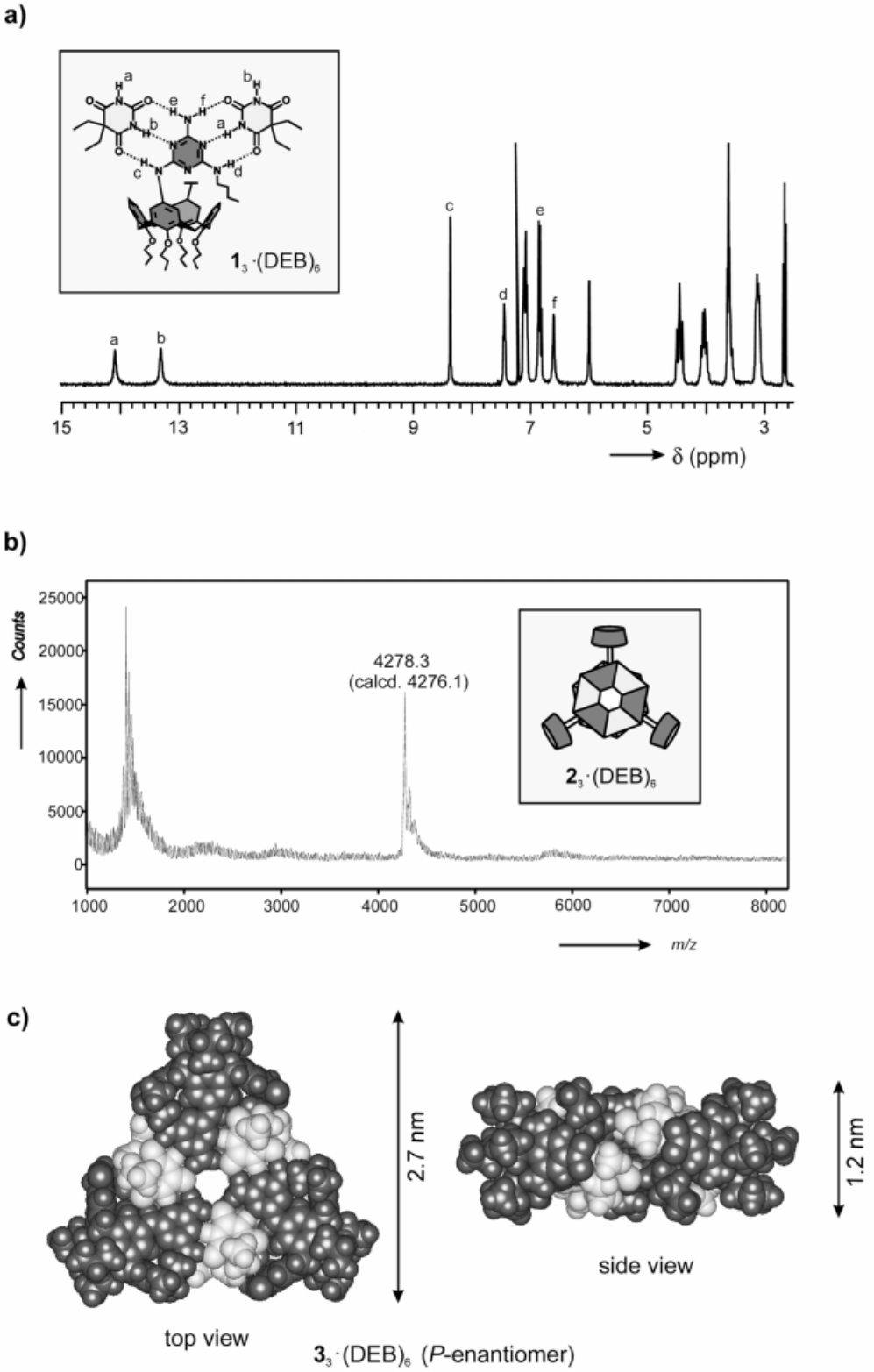

Figure 3. Characterization of calix[4]arene double rosette assemblies by a) ^{1}H NMR spectroscopy, b) MALDI-TOF mass spectrometry after Ag^I labelling, and c) X-ray crystallography

tensively using circular dichroism spectroscopy for the characterization of rosette assemblies (see Section 4.2 for details). This characterization technique is of tremendous value, particularly for thermodynamic stability measurements in polar solvents, in which NMR-spectroscopic studies are troublesome because of extensive proton exchange.

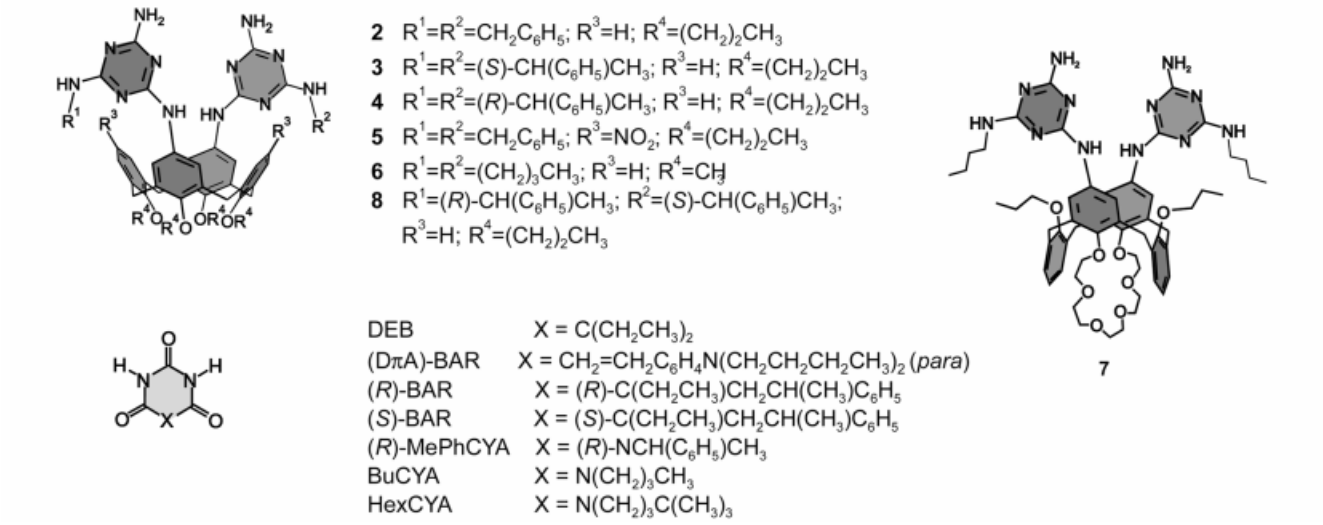

MALDI-TOF Mass Spectrometry after Ag^+ Labelling

Mass-spectrometric detection of hydrogen-bonded assemblies is usually very cumbersome, even when soft ionization methods such as ESI or MALDI are used. Only recently have several ion-labelling techniques been developed, greatly facilitating characterization by mass spectrometry.[31] In collaboration with Nibbering's group (University of Amsterdam), we have developed MALDI-TOF MS in combination with Ag^+ labelling, providing a nondestructive way to generate charged hydrogen-bonded assemblies that can be detected by mass spectrometry.[32] Using this method, we have successfully characterized over 25 different single, double, and quadruple rosette assemblies.[33] The method requires the presence of a suitable binding site for the Ag^+ ion. For example, when chloroform solutions (ca. 1 mM) of assemblies with aromatic side groups, such as $\mathbf{2}_3\cdot(DEB)_6$ (see Figure 3, b) or $\mathbf{3}_3\cdot(DEB)_6$ are treated with CF_3COOAg (ca. 1.5 equiv.) for 24 h at room temperature, intense signals are observed in the MALDI-TOF mass spectra at m/z = 4,278.3 [calcd. for $\mathbf{2}_3\cdot(DEB)_6\cdot{}^{107}Ag^+$ = 4,276.1] and 4,358.3 [calcd. for $\mathbf{3}_3\cdot(DEB)_6\cdot{}^{107}Ag^+$ = 4,360.2]. These and many other functionalities that provide strong binding sites for Ag^+ have been identified, acting either in a cooperative way (π-arene and π-alkene donor functionalities) or individually (cyano and crown ether functionalities). The method works well for assemblies with molecular weights between 2,000 and 8,000 Da. The MALDI-TOF MS data generally correlate very well with ^1H NMR spectroscopic data relating to the stability of these assemblies in solution.

X-ray Crystallography

Recrystallization of assembly $\mathbf{5}_3\cdot(DEB)_6$ from toluene gave large single crystals (5.0 × 5.0 × 5.0 mm) suitable for X-ray analysis. The crystal structure, which provides the first piece of evidence for the existence of double rosette assemblies in the solid state, shows that the two single rosette planes are neatly stacked on top of each other, with an interatomic distance of 3.2−3.5 Å (Figure 3, c). This leaves little space for complexation of guest molecules inside the assembly. Furthermore, it shows that the calix[4]arene units are fixed in a *pinched cone* conformation, the only conformation that allows simultaneous participation of the calix[4]arene units in both the upper and the lower rosette motifs.

3.3. Stability of Double Rosette Assemblies

Thermodynamic Studies

Calix[4]arene double rosette assemblies form spontaneously in apolar solvents ($CHCl_3$, CH_2Cl_2, toluene, benzene) upon mixing the separate components. The assembly process has a negative entropy (assembly of nine components), which is compensated for by the formation of 36 cooperative hydrogen bonds, resulting in an overall negative change of free energy (ΔG^0). Recent UV spectroscopy studies have shown that the thermodynamic stability is strongly solvent-dependent.[30] In chloroform, the assemblies start to dissociate at concentrations below 100 μM, while in benzene they are largely intact even at 5 μM concentrations. In the presence of polar solvents, the thermodynamic stabilities of the assemblies decrease rapidly and they start to dissociate. There is, however, a large difference in stability between barbituric acid based assemblies and their cyanuric acid based counterparts. For example, the $\chi_{THF/DCM}$ (% of THF at which 50% of the assembly in DCM is still intact)[34] for assembly $\mathbf{4}_3\cdot(DEB)_6$ is ca. 10%, while that of the corresponding assembly $\mathbf{4}_3\cdot(BuCYA)_6$ is ca. 95%. Similarly, the stabilities in the presence of DMSO also differ significantly ($\chi_{DMSO/CHCl_3}$ = 10% vs. 40%, respectively). These differences in thermodynamic stabilities are largely due to the increased acidity and basicity of the cyanurate donors and acceptors.[35,36]

The conformational fixing of the calix[4]arene skeleton is of crucial importance for the stability of the double rosette assembly. NMR diffusion measurements have shown that dimelamines like **6**, in which the calix[4]arene skeleton is

conformationally flexible, do not form stable double rosette assemblies, but instead give ill-defined polymeric networks.[29] On the other hand, dimelamine **7**, in which the calix[4]arene skeleton is fixed in the 1,3-alternate conformation, does give stable double rosettes. These results clearly show that it is proper preorganization of the melamine units, as in **1** and **7**, and not the bulkiness of the calix[4]arene fragment, that is primarily responsible for the clean formation of the double rosette assemblies.

Another way to improve the assembly stability is by covalently linking the calix[4]arene dimelamine and cyanurate units. On doing this, the number of separate components decreases from nine to three and the I_{Tm} value [$HB/(N-1)$, HB = number of hydrogen bonds, N = number of separate components] consequently rises from 4.5 to 18.[34] Assemblies with $\chi_{DMSO/CHCl_3}$ values of ca. 70% have been synthesized in this way.[37]

Kinetic Studies

Despite the fact that the hydrogen-bonded rosette assemblies are fully assembled in apolar solvents, there is a continuous exchange of individual components between the assemblies. This exchange process is also responsible for the self-correcting behaviour of the assemblies. The rate of the exchange processes depends strongly on the solvent and on the number of hydrogen bonds that have to be broken. Exchange of DEB fragments, which requires the breakage of only six hydrogen bonds, for example, is a relatively fast process ($k_d \approx 10^2-10^3$ s^{-1} in $CDCl_3$ at room temperature), while exchange of the dimelamines is much slower ($k_d \approx 10^{-1}-10^0$ s^{-1} in $CDCl_3$ at room temperature), since it involves the breakage of 12 hydrogen bonds (Scheme 2).

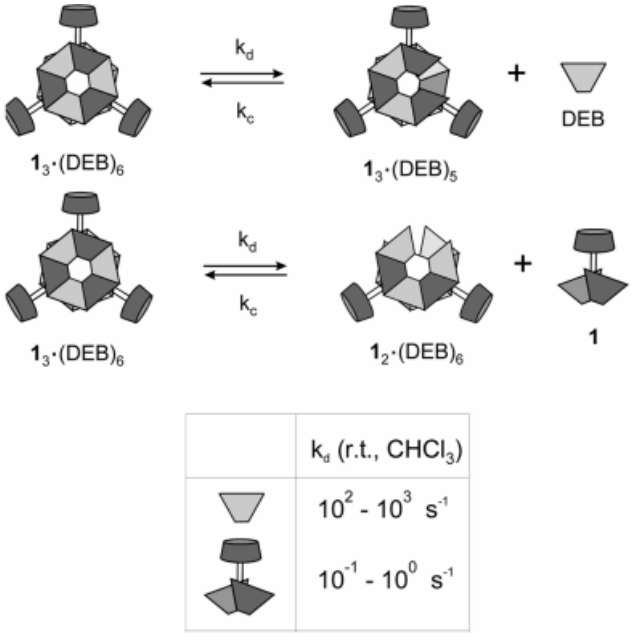

Scheme 2. Kinetic stabilities of calix[4]arene double rosette assemblies

4. Stereoselection: The Preferential Formation of *M* or *P* Diastereomers

Much to our surprise, we found that assembly $\mathbf{5}_3\cdot(DEB)_6$ exists in the solid state exclusively as the D_3 isomer, which displays chirality at the supramolecular level as a result of the *anti*-parallel orientation of the stacked rosette planes.[27] 2D NMR experiments using NOE spectroscopy also proved the exclusive existence of the D_3 isomer in solution. We termed the two mirror image assemblies the *P* and the *M* enantiomers, following the relative orientation of the two melamines at one calix[4]arene unit when viewing the assembly from the top, either clockwise (*P*) or counterclockwise (*M*).

4.1. Complete Induction of Supramolecular Chirality

We first studied the exclusive formation of one single helical form by attachment of chiral centres at the periphery of the assembly. Our general observation was that the introduction of chiral components results in asymmetric induction of supramolecular chirality in the assemblies.[38] At this stage the *P* and the *M* isomers are no longer mirror images, but instead have a *diastereomeric* relationship (see Figure 4), which means that they are not necessarily formed in equal quantities.

The degree of chiral induction is determined by the difference in the thermodynamic stabilities of the two diastereomers. Structural parameters such as proximity effects and the relative positioning of the chiral centres within the assembly primarily determine the relative stabilities of the two diastereomeric assemblies. However, the solvent also plays an important role here. Assembly of three molecules of dimelamine **5** and six molecules of chiral barbiturate (*R*)-BAR, in which the chiral carbon centre is two atoms remote from the barbituric acid ring (Figure 5), for example, gives a mixture of (*P*)-$\mathbf{5}_3\cdot[(R)\text{-BAR}]_6$ and (*M*)-$\mathbf{5}_3\cdot[(R)\text{-BAR}]_6$ with a diastereomeric excess (*de*) in $CDCl_3$ of 17% in favour of the *P* enantiomer.[39] The same assembly, however, displays a *de* of ca. 85% in [D_8]toluene, while in [D_6]benzene the diastereoselectivity is essentially complete (*de* > 98%). The extent of selectivity does not seem to be correlated with solvent polarity, as other assemblies exhibit far different solvent dependencies with respect to the observed diastereoselectivities.

When the chiral substituents are directly connected either to the nitrogen atom of the melamine units or to the cyanurate ring nitrogen atom, complete induction of chirality (*de* > 98%) has been observed in all cases.[38] For example, assembly of three units of chiral calix[4]arene dimelamine (*S*,*S*)-**3**, with (*S*)-1-phenylethyl substituents, with six units of DEB exclusively gives the *P* isomer of assembly $[(S,S)\text{-}\mathbf{3}]_3\cdot(DEB)_6$, as determined from the single set of signals in the ^{1}H NMR spectrum (see Figure 6). The corresponding $[(R,R)\text{-}\mathbf{4}]_3\cdot(DEB)_6$ assembly, with (*R*)-1-phenylethyl substituents, is formed exclusively as the *M* isomer. 2D NMR experiments using ROE spectroscopy have been used to cor-

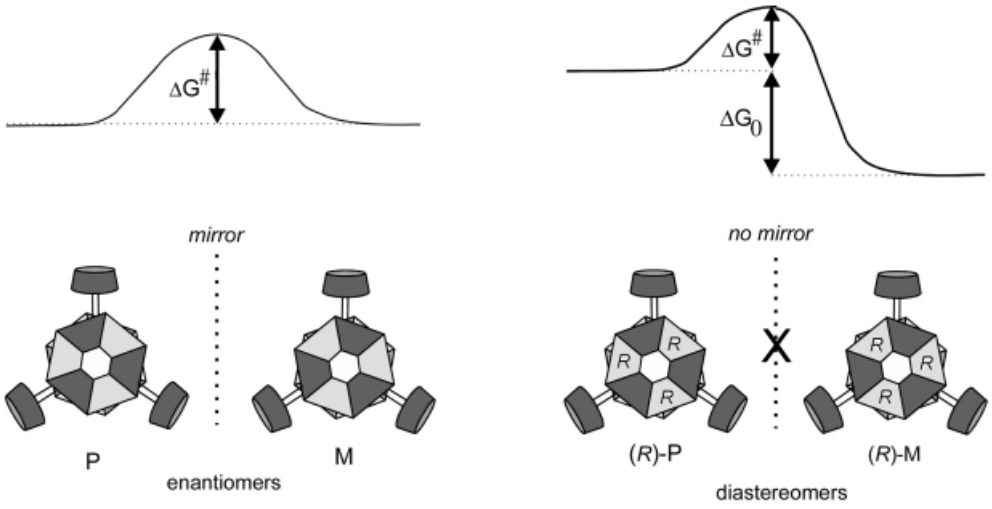

Figure 4. Enantiomerism and diastereoisomerism in double rosette assemblies

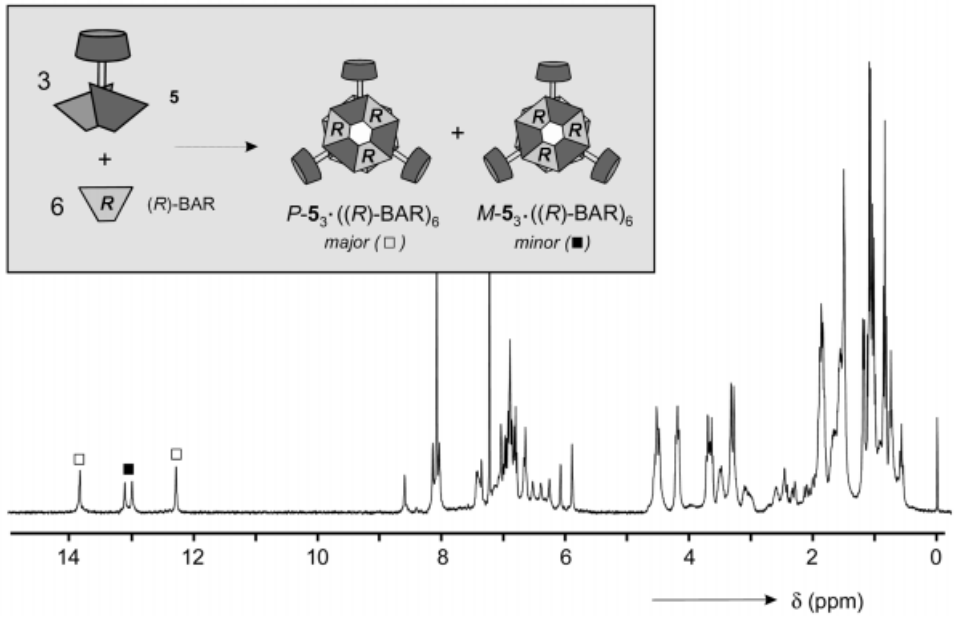

Figure 5. Noncovalent synthesis and characterization of assembly $\mathbf{5}_3$·[(*R*)-BAR)]$_6$

relate the absolute configurations of the substituents with the helicity of the assembly (see Figure 7). In a similar fashion, assembly of achiral dimelamine **2** and chiral (*R*)-MePhCYA gives rise to the exclusive formation of chiral assembly (*P*)-$\mathbf{2}_3$·[(*R*)-MePhCYA]$_6$ (see Figure 8).

The chiral components (*S*,*S*)-**3** and (*R*,*R*)-**4** display high degrees of *enantioselective* self-resolution; i.e., both components preferentially form the homomeric assemblies. No formation of the heteromeric assemblies was observed when the chiral assemblies (*P*)-[(*S*,*S*)-**3**]$_3$·(DEB)$_6$ and (*M*)-[(*R*,*R*)-**4**]$_3$·(DEB)$_6$ were mixed under conditions allowing reversible exchange of components **3** and **4**.

4.2. CD Spectroscopy Studies

Interestingly, the chiral double rosette assemblies display highly characteristic CD spectra (see Figure 6 and Figure 8), while the individual components are hardly CD-active ($\Delta\varepsilon_{max} < 8$ cm^2·mmol^{-1}). This clearly proves that the observed CD is a direct result of assembly formation and is not an intrinsic property of the individual components. The CD spectra of the assemblies typically display bisignate curves with remarkably large amplitudes ($\Delta\varepsilon_{max} \approx 100$ cm^2·mmol^{-1}). The peripheral chromophores (benzyl, carbonyl, naphthyl) only seem to affect the intensity of the

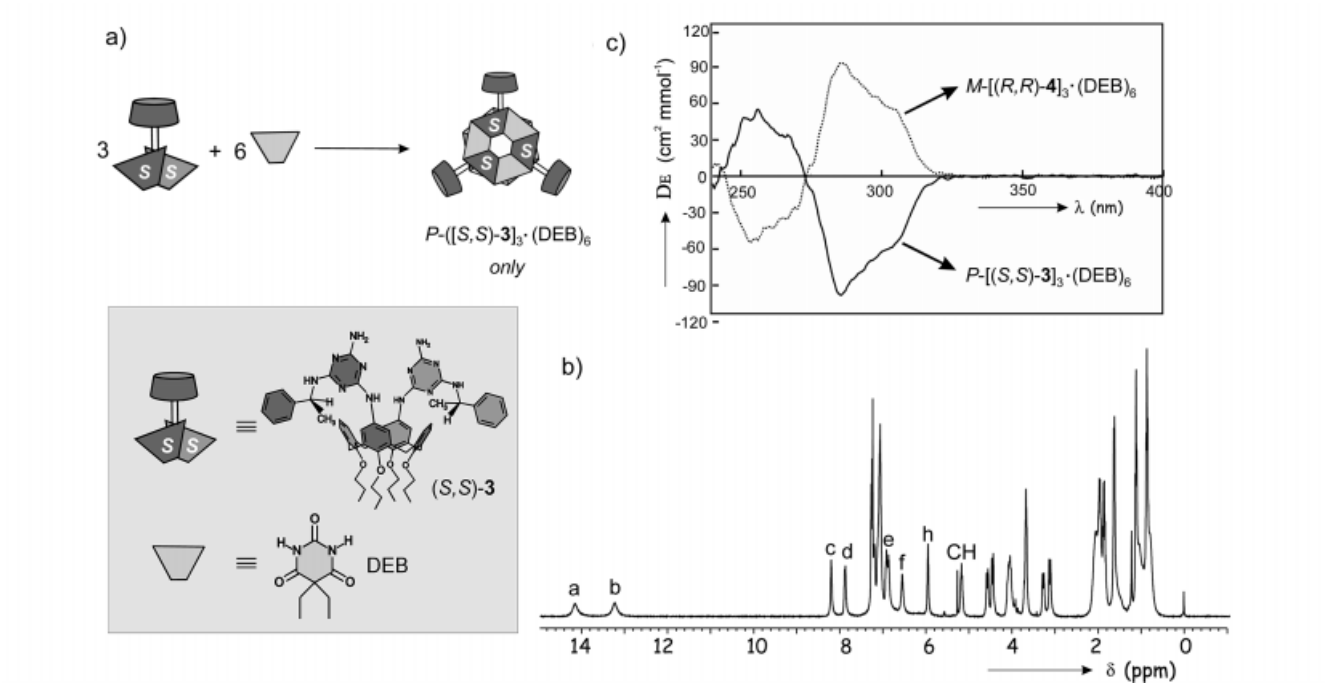

Figure 6. Diastereoselective noncovalent synthesis and characterization of assemblies (*P*)-[(*S*,*S*)-**3**]$_3$·(DEB)$_6$ and (*M*)-[(*R*,*R*)-**4**]$_3$·(DEB)$_6$

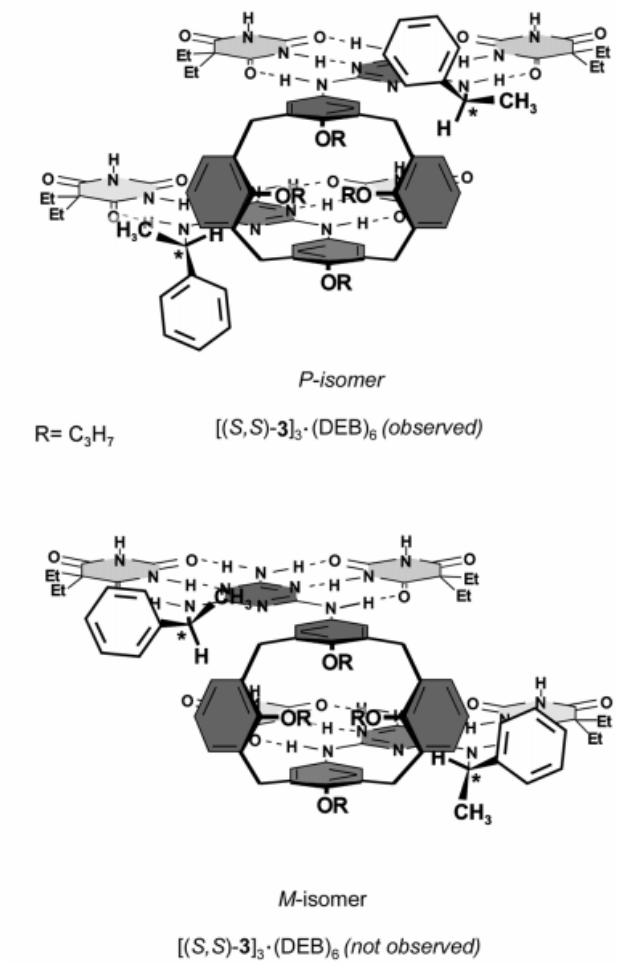

Figure 7. 2D ROESY analysis of assembly (*P*)-[(*S*,*S*)-**3**]$_3$·(DEB)$_6$

Cotton effect at lower wavelengths, while the observed CDs are virtually identical above 250 nm. Furthermore, the sign of the CD curve is a good measure of the helicity of the assembly. *M* enantiomers give positive CD curves, while *P* enantiomers give negative curves. CD spectroscopy is currently actively in use in our group for stability studies of double rosette assemblies in solution.

4.3. Cumulative Effects

Why exactly do the chiral substituents in **3** and **4** completely induce supramolecular chirality in the assembly? This can readily be understood by considering the microenvironment of the chiral substituent within the assembly (see Figure 7). By definition, two chiral substituents of opposite handedness, (*R*) and (*S*), have unequal energies in a chiral environment, because the mutual interactions with the chiral environment are diastereomeric in nature. For this reason, the (*S*) substituents in **3** will slightly favour the chiral microenvironment in the *P* enantiomer over the mirror image environment in the corresponding *M* enantiomer. In the staggered D_3 isomer, each chiral group experiences the same chiral microenvironment, which means that the individual energy difference ($\Delta H_{R/S}$) for each chiral substituent is cumulative, resulting in a total energy difference of $\Delta H_{total} \approx 6\ \Delta H_{R/S}$.

The impact of changing the absolute configuration of the chiral centres immediately becomes clear if the assembly behaviour of *meso* component (*R*,*S*)-**8** is considered (see Figure 9, c). In this component, the absolute configuration of half of the chiral centres is reversed with respect to (*R*,*R*)-**4**. Formation of the staggered D_3 isomer of assembly [(*R*,*S*)-**8**]$_3$·(DEB)$_6$ would position half of the chiral substituents in the energetically favourable environment, while the other

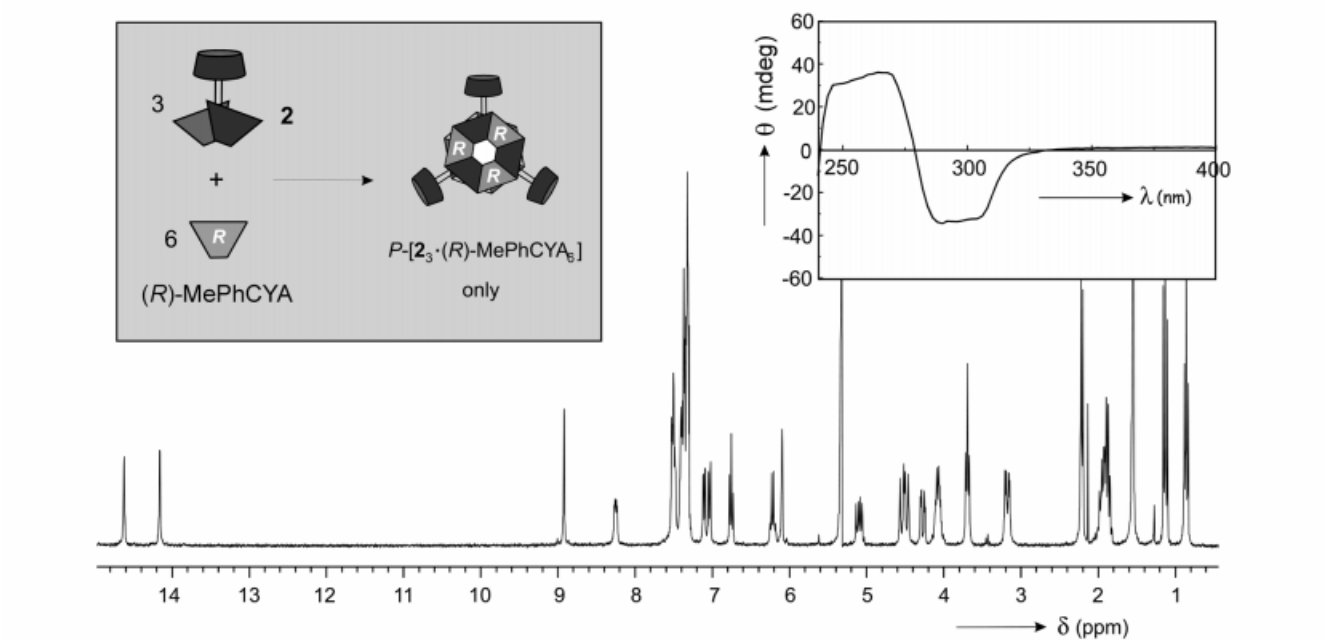

Figure 8. Noncovalent synthesis and characterization of assembly (*P*)-$\mathbf{2}_3$·[(*R*)-MePhCYA]$_6$

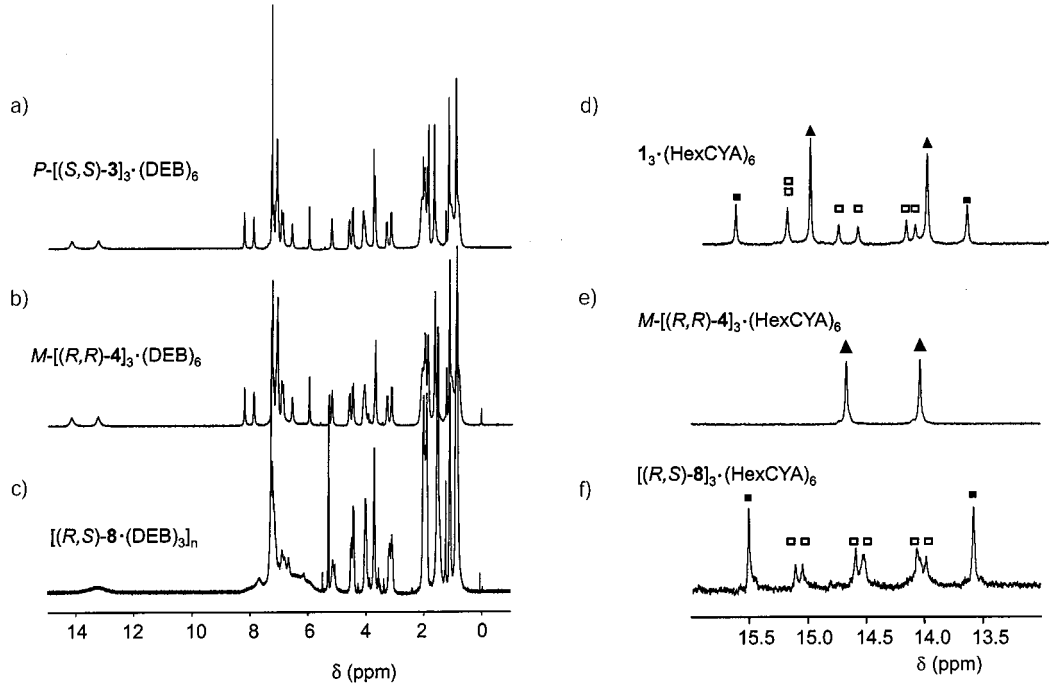

Figure 9. Regioselectivity in the assembly behaviour of achiral dimelamine **1**, chiral dimelamines (*S*,*S*)-**3** and (*R*,*R*)-**4**, and *meso*-dimelamine (*R*,*S*)-**8** (▲ indicates the proton signals for the D_3 isomer, ■ those for the C_{3h} isomer, and □ those for the C_s isomer)

chiral centres would be forced into the energetically unfavourable environment. As a consequence, formation of assembly [(*R*,*S*)-**8**]$_3$·(DEB)$_6$ does not occur, but undefined oligomers are formed instead.

5. Regioselectivity: The Preferential Formation of *Staggered* and *Eclipsed* Isomers

The chiral information in (*S*,*S*)-**3** and (*R*,*R*)-**4** can also be used to direct the formation of different isomers of the assembly. Typically, assemblies consisting of achiral dimelamines and cyanurates, such as $\mathbf{1}_3$·(HexCYA)$_6$, exist as mixtures of the chiral *staggered* isomer (D_3) and the two achiral *eclipsed* isomers (C_{3h} and C_s) (see Figure 2). The ^{1}H NMR spectrum of assembly $\mathbf{1}_3$·(HexCYA)$_6$ features ten different signals in the $\delta = 14-16$ region, two signals each for the D_3 and the C_{3h} isomers, and six different signals for the C_s isomer (Figure 9, d). However, when the achiral dimelamine **1** is substituted for one of the chiral components (*S*,*S*)-**3** or (*R*,*R*)-**4**, both of which possess two chiral centres of *iden-*

tical configuration, or (*R*,*S*)-**8**, which contains two chiral centres of *opposite* configuration, the isomeric distribution is changed dramatically. Assembly (*M*)-[(*R*,*R*)-**4**]$_3$·(HexCYA)$_6$, for example, exclusively exists as the chiral *staggered* D_3 isomer according to the two signals in the δ = 14−16 region of the ^{1}H NMR spectrum (see Figure 9, e). Not a trace of the two *eclipsed* isomers (C_{3h} and C_s) is observed. In analogy to this, assembly [(*R*,*S*)-**8**]$_3$·(HexCYA)$_6$, incorporating the *meso* component (*R*,*S*)-**8**, exists exclusively as a mixture of the two *eclipsed* isomers (C_{3h} and C_s). The staggered D_3 isomer is entirely absent and so the ^{1}H NMR spectrum displays only eight signals in the δ = 14−16 region (see Figure 9, f).

6. Enantioselection: The First "Enantiomerically Pure" Hydrogen-Bonded Assembly

There are many different hydrogen-bonded structures that display chirality at the supramolecular level. However, there is no reported example of an enantiomerically pure hydrogen-bonded assembly, presumably because of the very rapid racemization of these kinetically labile structures. This prompted us to attempt the enantioselective synthesis of double rosette assemblies and subsequently to study the mechanism and rate of racemization.

As mentioned, double rosette assemblies such as **1**$_3$·(BuCYA)$_6$ exist in the absence of peripheral chiral centres as racemic mixtures of the *M* and the *P* enantiomers (see Figure 4).[27] Intuitively, one would think that racemization of the two enantiomers would just be a matter of slipping the two rosette planes with respect to each other. This, however, is not the case, since the three calix[4]arene units serve as "lockers", preventing rotatory slippage of the individual rosettes. It therefore seems likely that interconversion of the *P* enantiomer of **1**$_3$·(BuCYA)$_6$ into the *M* enantiomer and vice versa requires the breakage of multiple hydrogen bonds. On this presumption, the energy barrier for racemization should be significantly higher than otherwise expected for a noncovalent assembly exclusively held together by weak interactions.

For the synthesis of enantiomerically pure double rosette assemblies, we make use of the large difference in stabilities between M·CA and M·BA complexes (see Figure 10). For example, the K_{ass} of the 1:1 complex **9·10** is ca. 2,200 M^{-1},

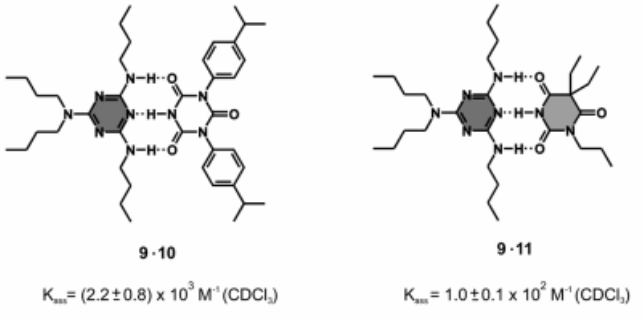

Figure 10. Relative stabilities of the melamine−cyanuric and melamine−barbituric acid complexes **9·10** and **9·11**

roughly 20-fold higher than that of the 1:1 complex **9·11**, with a K_{ass} of ca. 100 M^{-1}.[39] As a consequence, the barbituric acid components in assembly **1**$_3$·(DEB)$_6$ can be quantitatively substituted for cyanuric acid components, simply by addition of free cyanurate to the assembly.

The enantioselective synthesis of assemblies (*M*)-**1**$_3$·(BuCYA)$_6$ and (*P*)-**1**$_3$·(BuCYA)$_6$ starts with the diastereoselective formation of assemblies (*M*)-**1**$_3$·[(*R*)-BAR]$_6$ and (*P*)-**1**$_3$·[(*S*)-BAR]$_6$. While in $CDCl_3$ these assemblies are formed only with a slight excess of one of the diastereomers (*de* = 17%), their formation in [D$_6$]benzene occurs with complete diastereoselectivity (*de* > 98%), as determined from the single set of proton signals at δ = 12.69 and 14.46 in the ^{1}H NMR spectrum.[39] Moreover, the circular dichroism spectra are highly characteristic of calix[4]arene double rosette assemblies and reflect the opposite handedness of the assemblies. The chiral barbiturates in (*M*)-**1**$_3$·[(*R*)-BAR]$_6$ and (*P*)-**1**$_3$·[(*S*)-BAR]$_6$ are subsequently substituted for achiral cyanurates upon the addition of BuCYA. At a 1:1.2 ratio of (*R*)-BAR [or (*S*)-BAR] to BuCYA the exchange process is quantitative, as judged from the appearance of a new set of proton signals at δ = 14.42 and 14.89 and the complete disappearance of the other two signals (see Figure 11). Moreover, MALDI-TOF mass spectrometry after Ag^I labelling of the crude mixture also confirms the complete exchange of the chiral barbiturates for achiral cyanurates. The resulting assemblies (*M*)-**1**$_3$·(BuCYA)$_6$ and (*P*)-**1**$_3$·(BuCYA)$_6$ still have very strong CDs ($\Delta\varepsilon_{max} \approx 90$ $cm^2 \cdot mmol^{-1}$), indicating that the assembly has memorized the chirality that was induced in the presence of the chiral barbiturates. Independent ^{1}H NMR experiments have shown that no racemization occurs during the exchange process, which proves that the optical purities of assemblies (*M*)-**1**$_3$·(BuCYA)$_6$ and (*P*)-**1**$_3$·(BuCYA)$_6$ must be similar to those of their precursor assemblies: i.e., *ee* > 98%.

Assemblies (*M*)-**1**$_3$·(BuCYA)$_6$ and (*P*)-**1**$_3$·(BuCYA)$_6$ provide the first examples of hydrogen-bonded assemblies in an optically pure state. We studied their racemization at different temperatures using CD spectroscopy and found a remarkably high energy barrier of 105.9 $kJ \cdot mol^{-1}$, corresponding to a lifetime of ca. 4.5 d in benzene at room temperature. Kinetic studies showed that there are two different pathways for racemization: by regular dissociation of the assembly with loss of chiral memory, and by a similar dissociative pathway in which the liberated (*R*)-BAR acts as a catalyst (see Figure 12). Both processes are first order in assembly (*M*)-**1**$_3$·(BuCYA)$_6$ and are characterized by the rate constants $k_{uncat} = 1.1 \cdot 10^{-5}$ s^{-1} and $k_{cat} = 7.4 \cdot 10^{-3}$ $L \cdot mol^{-1} \cdot s^{-1}$ (50 °C).

7. Self-Organization on Surfaces: Spontaneous Formation of Nanotubes

The self-assembly of low molecular weight building blocks into *noncovalent* polymeric nanostructures has recently attracted considerable interest for applications in nanotechnology as a *bottom-up* approach for the construc-

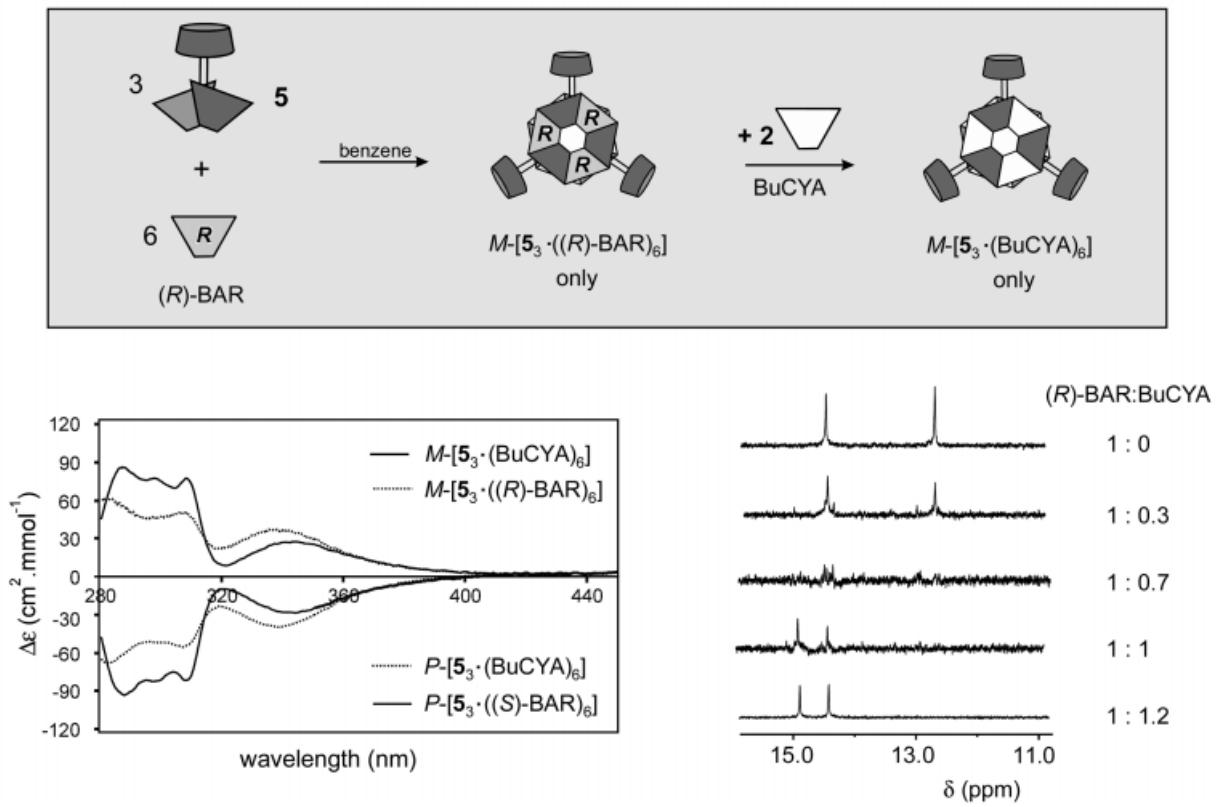

Figure 11. Enantioselective noncovalent synthesis and characterization of assembly (*M*)-$\mathbf{5}_3$·$(BuCYA)_6$

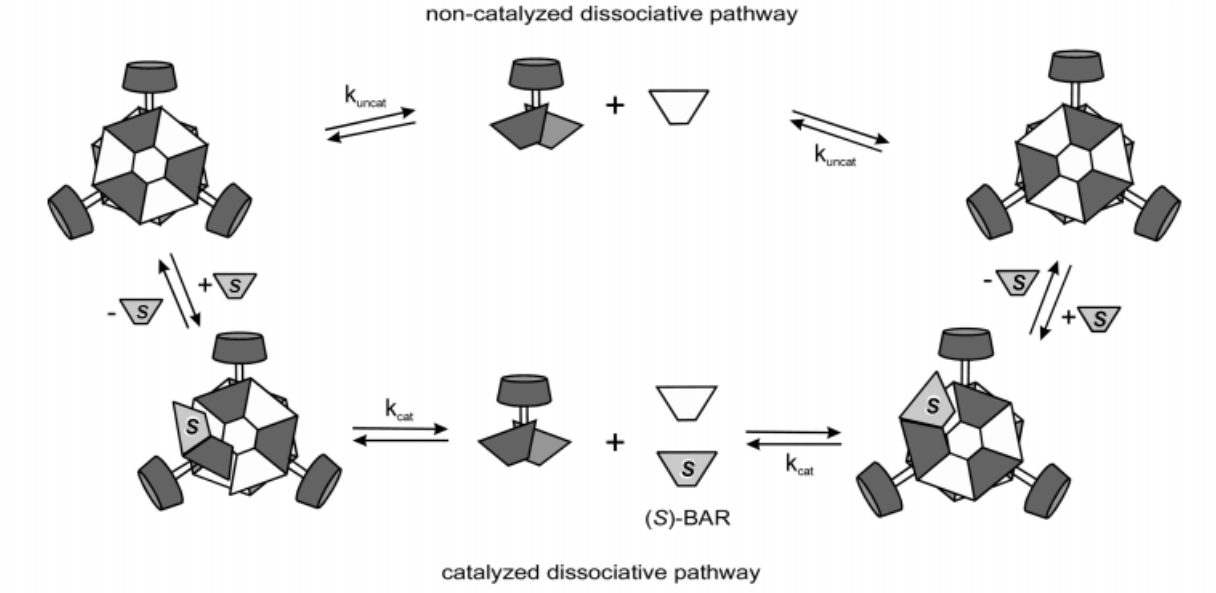

Figure 12. Two different mechanisms for the racemization of assembly (*M*)-$\mathbf{5}_3$·$(BuCYA)_6$

tion of molecular scale devices. In the light of this, we studied the self-organization of assembly $\mathbf{1}_3$·$(DEB)_6$ on graphite by TM-SFM. It was found that the assemblies form linear, rod-like structures on the surface.[40] Formation of similar rod-like structures was never observed in solution, not even at very high concentration. The rod-like structures are most probably formed by face-to-face arrangement of multiple disk-like assemblies $\mathbf{1}_3$·$(DEB)_6$, in a process driven by solvophobic interactions. Unfortunately, it has so far not been possible to study the chirality of the rod-like structures, not even by STM, because of insufficient image resolution.

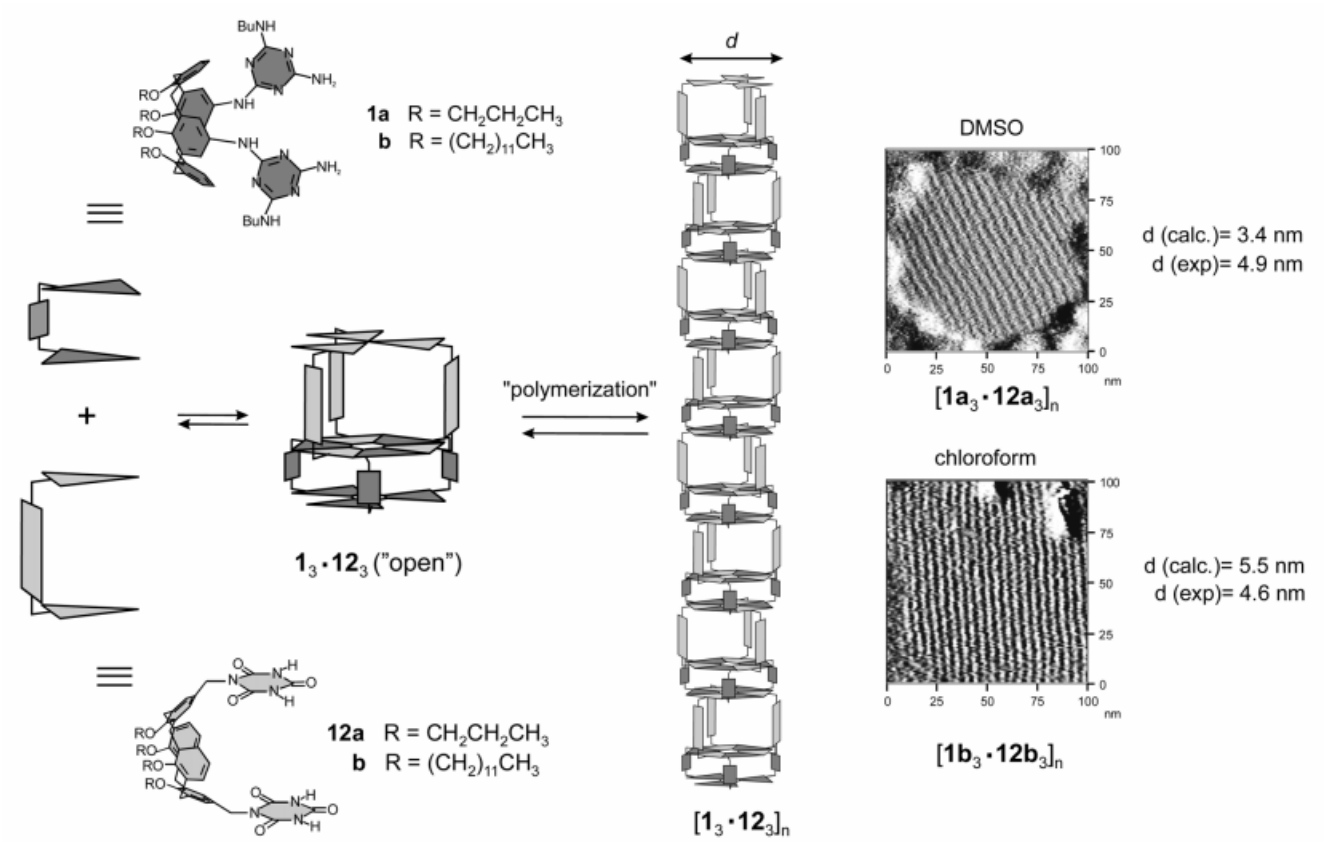

Figure 13. TM-SFM analysis of rod-like nanostructures $[\mathbf{1}_3\cdot\mathbf{12}_3]_n$ on graphite

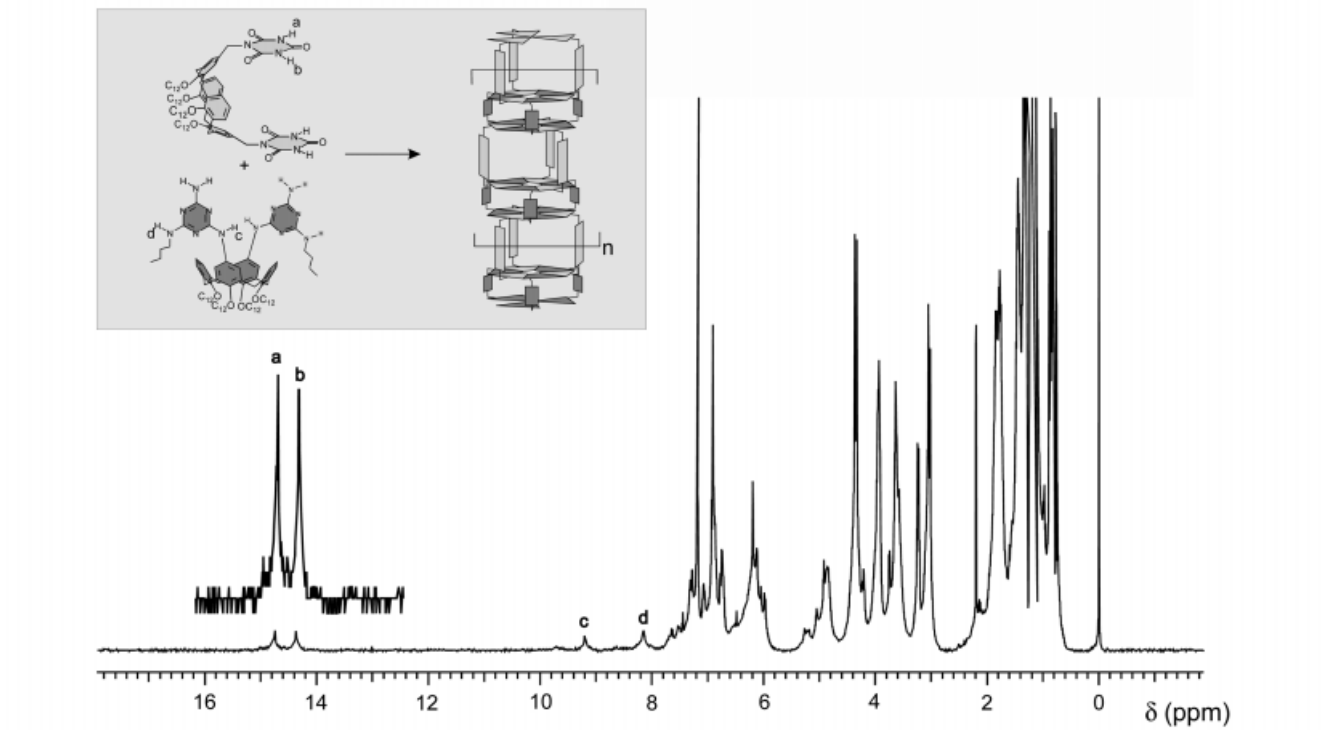

Figure 14. ^{1}H NMR characterization of polymeric assembly $[\mathbf{1}_3\cdot\mathbf{12}_3]_n$ in solution

In order to produce noncovalent polymeric nanostructures also capable of being formed in solution, we investigated the self-organization of ''non-matching'' calix[4]arene dimelamine **1** and calix[4]arenebis(cyanuric acid) **12** (Figure 13). It is postulated that **1** and **12** initially form the ''open'' structure $[\mathbf{1}_3\cdot\mathbf{12}_3]$, the top of which is complement-

ary to the bottom. Hydrogen bond directed polymerization of this structure subsequently results in the formation of rod-like nanostructures $[\mathbf{1}_3{\cdot}\mathbf{12}_3]_n$.

These structures are indeed formed, both in solution and on a graphite substrate. TM-SFM analysis of the polymers $[\mathbf{1}_3{\cdot}\mathbf{12}_3]_n$ showed perfectly aligned linear strands with dimensions between 3.5 and 5.5 nm, forming regular patterns across the surface (see Figure 13). The dimensions of the structures show good correlations with model calculations, indicating that the structures are densely packed on the substrate. No formation of these structures was observed in control experiments with separate solutions of the individual components.

The more hydrophobic nanostructure is sufficient soluble in apolar solvents to be characterized by spectroscopy. The ^{1}H NMR spectrum of the polymeric nanostructure $[\mathbf{1b}_3{\cdot}\mathbf{2b}_3]_n$ shows the diagnostic signals for double rosette formation (Figure 14). In particular, the single set of imide proton signals at $\delta = 14.8$ and 14.4 provides strong evidence for the presence of only one type of hydrogen-bonded assembly.

8. Conclusions

The hydrogen bond directed formation of double rosette assemblies provides an illustrative example of the structural complexity and diversity that can be accomplished using noncovalent synthesis with the aid of hydrogen bonding. Typical concepts originating from the covalent world, such as stereoselective, regioselective, and enantioselective synthesis, have been studied and it has been learned that the cooperative action of the individual components provides the key to the high stereoselectivities that may be observed in these systems. These noncovalent assemblies also show self-assembling behaviour on a higher level, giving access to well-defined structures of nanometer dimensions.

Acknowledgments

The authors would like to acknowledge the contributions of Kate Jolliffe, Jean-Luc Weidmann, Mercedes Crego Calama, Chris Marjo, Harm-Anton Klok, Caroline Schauer, Francesca Cardullo, Ron Hulst, Roel Fokkens, Nico Nibbering, Feike de Jong, and David Reinhoudt for their active participation in the work presented in this article. Financial support from CW-NWO, JST and EC is also gratefully acknowledged.

[1] R. W. Armstrong, J.-M. Beau, S. H. Cheon, W. J. Christ, H. Fujioka, W. H. Ham, L. D. Hawkins, H. Jin, S. H. Kang, Y. Kishi, M. J. Martinella, W. W. McWhorter, M. Mizuno, M. Nakata, A. E. Stutz, F. X. Talamas, M. Taniguchi, J. A. Tino, K. Ueda, J. Uenishi, J. B. White, M. Yonaga, *J. Am. Chem. Soc.* **1989**, *111*, 7525−7530.
[2] K. C. Nicolaou, R. K. Guy, *Angew. Chem.* **1995**, *107*, 2047−2059; *Angew. Chem. Int. Ed. Engl.* **1995**, *34*, 2079−2090.
[3] J. J. Masters, J. T. Link, L. B. Snyder, W. B. Young, S. J. Danishefsky, *Angew. Chem.* **1995**, *107*, 1886−1888; *Angew. Chem. Int. Ed. Engl.* **1995**, *34*, 1723−1726.
[4] K. C. Nicolaou, *Angew. Chem.* **1996**, *108*, 644−664; *Angew. Chem. Int. Ed. Engl.* **1996**, *35*, 589−607.
[5] We specifically refer here to the stepwise synthesis of small molecules. It should be made clear that this does not include any type of (bio)polymerization reactions, which obviously afford easy access to high molecular weight structures.
[6] L. J. Prins, P. Timmerman, D. N. Reinhoudt, *Angew. Chem. Int. Ed.* **2001**, *40*, 2382−2426.
[7] G. M. Whitesides, E. E. Simanek, J. P. Mathias, C. T. Seto, D. N. Chin, M. Mammen, D. M. Gordon, *Acc. Chem. Res.* **1995**, *28*, 37−44.
[8] S. Pennazio, P. Roggero, *Riv. Biol.* **1999**, *92*, 289−323.
[9] M. Fujita, K. Ogura, *Bull. Chem. Soc. Jpn.* **1996**, *69*, 1471−1482.
[10] C. Piguet, G. Bernardinelli, G. Hopfgartner, *Chem. Rev.* **1997**, *97*, 2005−2062.
[11] M. Alamgir Hossain, H.-J. Schneider, *Chem. Eur. J.* **1999**, *5*, 1284−1290.
[12] W. Blokzijl, J. B. F. N. Engberts, *Angew. Chem.* **1993**, *105*, 1610−1644; *Angew. Chem. Int. Ed. Engl.* **1993**, *32*, 1545−1579.
[13] M. Rekharsky, Y. Inoue, *Chem. Rev.* **1998**, *98*, 1875−1917.
[14] A. Ranganathan, V. R. Pedireddi, C. N. R. Rao, *J. Am. Chem. Soc.* **1999**, *121*, 1752−1753.
[15] J.-M. Lehn, M. Mascal, A. DeCian, J. Fischer, *J. Chem. Soc., Chem. Commun.* **1990**, 479−480.
[16] C. T. Seto, G. M. Whitesides, *J. Am. Chem. Soc.* **1990**, *112*, 6409−6411.
[17] J. A. Zerkowski, C. T. Seto, G. M. Whitesides, *J. Am. Chem. Soc.* **1992**, *114*, 5473−5475.
[18] C. M. Drain, K. C. Russell, J.-M. Lehn, *Chem. Commun.* **1996**, 337−338.
[19] J. A. Zerkowski, C. T. Seto, D. A. Wierda, G. M. Whitesides, *J. Am. Chem. Soc.* **1990**, *112*, 9025−9026.
[20] J. A. Zerkowski, G. M. Whitesides, *J. Am. Chem. Soc.* **1994**, *116*, 4298−4304.
[21] J. P. Mathias, E. E. Simanek, J. A. Zerkowski, C. T. Seto, G. M. Whitesides, *J. Am. Chem. Soc.* **1994**, *116*, 4316−4325.
[22] J. P. Mathias, E. E. Simanek, G. M. Whitesides, *J. Am. Chem. Soc.* **1994**, *116*, 4326−4340.
[23] A. G. Bielejewska, C. E. Marjo, L. J. Prins, P. Timmerman, F. De Jong, D. N. Reinhoudt, *J. Am. Chem. Soc.*, accepted.
[24] X. Chi, A. J. Guerin, R. A. Haycock, C. A. Hunter, L. A. Sarson, *J. Chem. Soc., Chem. Commun.* **1995**, 2563−2565.
[25] G. Ercolani, *J. Phys. Chem. B* **1998**, *102*, 5699−5703.
[26] R. H. Vreekamp, J. P. M. Van Duynhoven, M. Hubert, W. Verboom, D. N. Reinhoudt, *Angew. Chem.* **1996**, *108*, 1306−1309; *Angew. Chem. Int. Ed. Engl.* **1996**, *35*, 1215−1218.
[27] P. Timmerman, R. H. Vreekamp, R. Hulst, W. Verboom, D. N. Reinhoudt, K. Rissanen, K. A. Udachin, J. Ripmeester, *Chem. Eur. J.* **1997**, *3*, 1823−1832.
[28] L. J. Prins, K. A. Jolliffe, R. Hulst, P. Timmerman, D. N. Reinhoudt, *J. Am. Chem. Soc.* **2000**, *122*, 3617−3627.
[29] P. Timmerman, J.-L. Weidmann, K. A. Jolliffe, L. J. Prins, D. N. Reinhoudt, S. Shinkai, L. Frish, Y. Cohen, *J. Chem. Soc., Perkin Trans. 2* **2000**, 2077−2089.
[30] L. J. Prins, C. Thalacker, F. Wurthner, P. Timmerman, D. N. Reinhoudt, *Proc. Natl. Acad. Sci. USA*, accepted.
[31] C. A. Schalley, *Int. J. Mass Spectr.* **2000**, *194*, 11−39.
[32] K. A. Jolliffe, M. Crego Calama, R. Fokkens, N. M. M. Nibbering, P. Timmerman, D. N. Reinhoudt, *Angew. Chem.* **1998**, *110*, 1294−1297. *Angew. Chem. Int. Ed.* **1998**, *37*, 1247−1251.
[33] P. Timmerman, K. A. Jolliffe, M. Crego Calama, J.-L. Weidmann, L. J. Prins, F. Cardullo, B. H. M. Snellink-Ruel, R. Fokkens, N. M. M. Nibbering, S. Shinkai, D. N. Reinhoudt, *Chem. Eur. J.* **2000**, 4104−4115.

[34] M. Mammen, E. E. Simanek, G. M. Whitesides, *J. Am. Chem. Soc.* **1996**, *118*, 12614−12623.
[35] H. S. Shieh, D. Voet, *Acta Crystallogr., Sect. B: Struct. Sci.* **1976**, *32*, 2354−2360.
[36] M. Mascal, P. S. Fallon, A. S. Batsanov, B. R. Heywood, S. Champ, M. Colclough, *J. Chem. Soc., Chem. Commun.* **1995**, 805−806.
[37] O. Felix, I. Luyten, P. Timmerman, D. N. Reinhoudt, manuscript in preparation.
[38] L. J. Prins, J. Huskens, F. De Jong, P. Timmerman, D. N. Reinhoudt, *Nature (London)* **1999**, *398*, 498−502.
[39] L. J. Prins, F. De Jong, P. Timmerman, D. N. Reinhoudt, *Nature (London)* **2000**, *408*, 181−184.
[40] H.-A. Klok, K. A. Jolliffe, C. L. Schauer, L. J. Prins, J. P. Spatz, M. Moller, P. Timmerman, D. N. Reinhoudt, *J. Am. Chem. Soc.* **1999**, *121*, 7154−7155.

Received March 23, 2001
[O01137]